Electrochemical and X-Ray Crystallographic Studies on three Macrocyclic Dicopper(I) Complexes†

Paul C. Yates,[a] **Michael G. B. Drew,***[a] **Jadwiga Trocha-Grimshaw,**[b] **Kieran P. McKillop,**[b] **S. Martin Nelson,**[b] **Peter T. Ndifon,**[c] **Charles A. McAuliffe**[c] **and Jane Nelson***[d]
[a] *The University, Whiteknights, Reading RG6 2AD, UK*
[b] *Queens University of Belfast, Belfast BT9 5AG, UK*
[c] *UMIST, Manchester M60 1QD, UK*
[d] *Open University, 40 University Road, Belfast BT7 1SU, UK*

The crystal structures of the compounds $[Cu_2L^1(NCMe)_2][BPh_4]_2$ **1′**, $[Cu_2L^2(NCMe)_2][ClO_4]_2$ **2** and $[Cu_2L^3(NCMe)_2][ClO_4]_2$ **3** have been determined {L^1 = 23,24-dioxa-3,7,14,18-tetraazatricyclo-[18.2.1.1^{9,12}]tetracosa-1(22),2,7,9,11,13,18,20-octaene, L^2 = 5,5,16,16-tetramethyl derivative of L^1, L^3 = 23,24-dithia analogue of L^1}. Complex **1′** is monoclinic, space group $P2_1/n$, $Z = 2$ with a = 10.45(1), b = 15.72(1), c = 18.08(1) Å and β = 97.0(1)°, **2** is triclinic, space group $P\bar{1}$, $Z = 1$, with a = 7.447(8), b = 12.094(9), c = 10.731(9) Å, α = 118.6(1), β = 78.8(1) and γ = 103.7(1)° and **3** is monoclinic, space group $P2_1/c$, $Z = 2$, with a = 8.15(1), b = 9.41(1), c = 19.35(2) Å and β = 100.0(1)°; 1122, 1298 and 1071 reflections have been refined to R 0.079, 0.055 and 0.072 respectively. All structures contain discrete cations and anions with the cations containing crystallographic centres of symmetry. In the cations the copper atoms are three-co-ordinate being bound to two nitrogen atoms of the macrocycle and one of an NCMe group in a pyramidal co-ordination sphere, Cu–N bond lengths ranging from 1.855(5) to 1.991(11) Å. The Cu···S distances in **3** are 3.07(1) and 2.89(1) Å indicating a fairly strong interaction. This distorts the planar part of the macrocycle and leads to a large Cu···Cu separation of 4.654(3) Å. The corresponding value of 3.675(1) Å in **2** is larger than that of 3.395(4) Å in **1** due to repulsion between the additional methyl groups in L^2.

Previous studies[1] of dicopper complexes of the macrocyclic ligands 23,24-dioxa-3,7,14,18-tetraazatricyclo[18.2.1.1^{9,12}]-tetracosa-1(22),2,7,9,11,13,18,20-octaene (L^1) and its 5,5,16,16-tetramethyl derivative (L^2) have revealed an active redox chemistry, including spontaneous reduction[2] of dicopper(II) complexes in acetonitrile solution, facile aerobic oxidation of dicopper(I) complexes in other solvents,[3] the existence of a mixed-valence dicopper(I,II) species,[4] together with catalytic activity in the dehydrogenation[2,3] and oxygenation[5] of organic substrates. We consider this borderline copper(I)/copper(II) stability to derive from a combination of electronic and geometric factors, arising respectively from co-ordination of 'soft' imino-donors and non-availability of the square-based geometry preferred by Cu^{II}. In an attempt to extend this interesting and potentially useful chemistry, we have prepared ligands L^3 and L^4 (the 23,24-dithia analogues of L^1 and L^2) where the substitution of the (presumed non-co-ordinating) thiophene for furan was expected to have (if any) geometric rather than electronic consequences, and thus have only marginal effect on the redox preferences of the co-ordinated metal ion.

It was immediately obvious, however, that this replacement had a major effect on the redox stability of co-ordinated copper(I). Both with L^3 and L^4 which was briefly studied for corroborative purposes, the +1 oxidation state was favoured to the extent that no aerobic oxidation was observed even in solvents such as dimethylacetamide (dma) or dimethylformamide (dmf) where $[Cu_2L^1]^{2+}$ and $[Cu_2L^2]^{2+}$ are rapidly oxidised[4] to a brown mixed-valence and subsequently green dicopper(II) form. An X-ray diffraction crystallographic study was therefore undertaken to see whether the macrocyclic geometry in $[Cu_2L^3]^{2+}$ could account for this difference in redox behaviour.

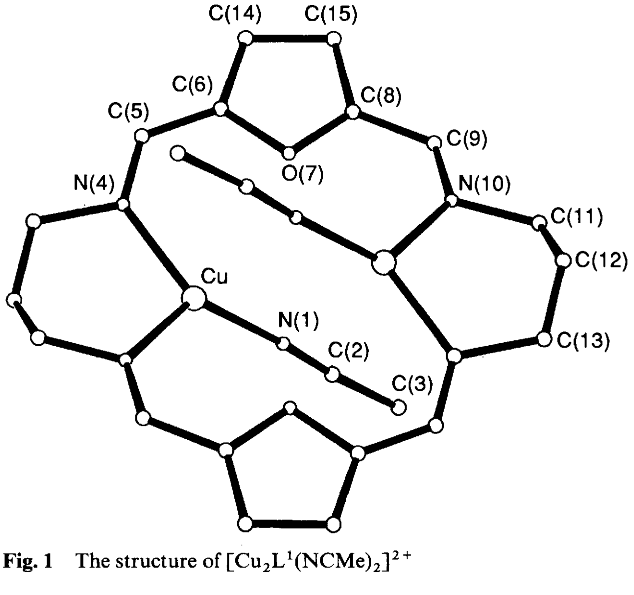

Fig. 1 The structure of $[Cu_2L^1(NCMe)_2]^{2+}$

Results and Discussion

The structures of complexes $[Cu_2L^1(NCMe)_2][BPh_4]_2$ **1′**, $[Cu_2L^2(NCMe)_2][ClO_4]_2$ **2** and $[Cu_2L^3(NCMe)_2][ClO_4]_2$ **3**

---

† *Supplementary data available:* see Instructions for Authors, *J. Chem. Soc., Dalton Trans.*, 1991, Issue 1, pp. xviii–xxii.

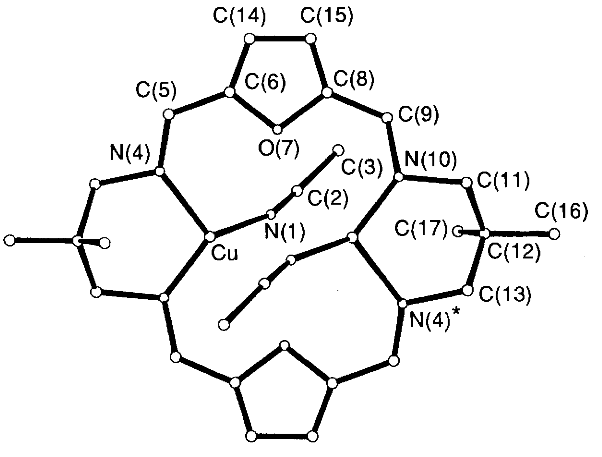

Fig. 2 The structure of $[Cu_2L^2(NCMe)_2]^{2+}$

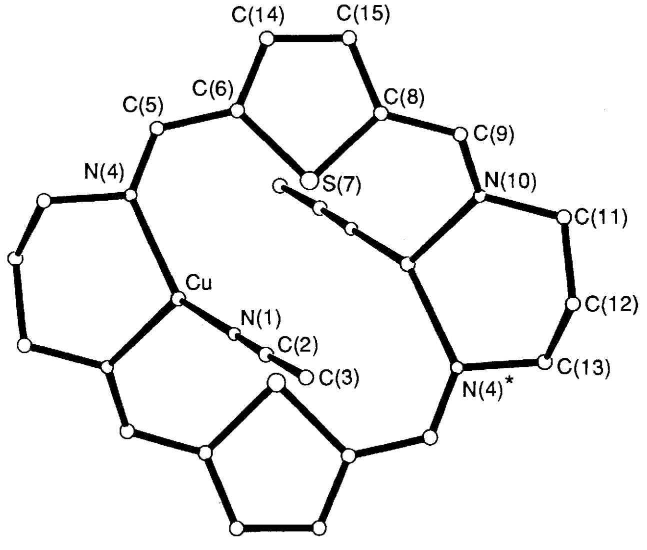

Fig. 3 The structure of $[Cu_2L^3(NCMe)_2]^{2+}$

all consist of discrete cations and anions. The cations are shown in Figs. 1, 2 and 3 respectively together with the common atomic numbering scheme. In each case the two halves of the cation are related by a centre of symmetry.

In each structure both copper atoms are three-co-ordinate, being bonded to two nitrogen atoms of the macrocycle and the nitrogen atom of the NCMe group. The Cu–N bond lengths to the NCMe group are significantly shorter [1.914(18), 1.872(13), 1.855(15) Å] in all three cases than those to the macrocycle [1.942(11)–1.991(11) Å]. All the co-ordination spheres exhibit a slight pyramidal distortion from planarity. There is a great variation in the Cu ··· Cu distances in each structure [3.395(4) for **1′**, 3.675(1) for **2** and 4.654(3) Å for **3**].

A substantial part of each macrocycle, that from N(4) through the five-membered ring to N(10), is planar as expected. The largest deviations within this region are quantified by values of $-17°$ for the O(7)–C(8)–C(9)–N(10) torsion angle in complex **1′** and -17 and $-13°$ for N(4)–C(5)–C(6)–O(7) and O(7)–C(8)–C(9)–N(10) in **2**. A much larger deviation is shown by the value of 30° for S(7)–C(8)–C(9)–N(10) in **3**, but the corresponding torsion angle on the opposite side of the ring, N(4)–C(5)–C(6)–S(7), has a value of 1° which is very close to that expected. This indicates that there are severe steric distortions of the macrocycle in **3**. In the other sections of each macrocycle the deviations from ideal values are generally greater and it appears that any strain is relieved in these parts of the structures. Least-squares-planes calculations given in Table 9 also highlight the deviation from planarity in **3** with N(10) lying 0.25 Å below the plane defined by this group of atoms.

It is possible that the oxygen or sulphur atom within the five-membered furan or thiophene ring may be involved in a weak interaction with the copper atoms. In complex **1′** the Cu ··· O distances are 2.95(1) and 2.78(1) Å which may represent a weak interaction as observed in another complex of this macrocycle, $[Cu_2L^1(dppm)]^{2+}$ [dppm = bis(diphenylphosphino)methane].[1,6] In **2** both distances are 3.05(1) Å which are relatively long and unlikely to be of great significance. However, in **3** the Cu ··· S contact distances are 3.07(1) and 2.89(1) Å which are quite comparable with the Cu ··· O distances quoted above. Given the larger size of the sulphur atom with respect to oxygen, it seems that there is a moderately strong Cu ··· S interaction which may be responsible for the distortions in the macrocycle of complex **3**. The distances quoted compare with 3.013 Å for a Cu^{II} ··· S[7] and 2.90 and 3.16 Å for Cu^{I} ··· S[8] contacts in other systems believed to contain thiophene-*S* co-ordinated to copper.

The shortest cation–anion contacts all have similar values in the three structures: C(14) ··· C(42) 3.26(3) Å in **1′**, C(3) ··· O(20) 3.16(3) Å in **2** and C(2) ··· O(22) 3.12(2) Å in **3**. The shortest contacts to other unit cells also involve cation–anion interactions and are no shorter than 3.22(3) Å.

A comparison of the three structures shows the effect of substituents on the macrocycle L^1. Introduction of methyl groups on C(12) results in additional repulsions between opposite sides of the macrocycle and an increased separation of the copper atoms. There is little change in the macrocycle conformation, but the orientation of the NCMe groups alters to accommodate these changes. Replacement of oxygen by sulphur in the five-membered rings results in more severe distortions in the macrocycle; the five-membered ring is pushed outwards leading to a copper–sulphur interaction which in turn produces distortions on one side of the macrocycle. Fig. 4 shows each cation projected onto the five-membered ring. The differences in NCMe orientation and the non-planar section of each macrocycle are clearly visible.

The similarity of the copper co-ordination site in complexes **1′** and **2** is reassuring, in view of the very similar chemical behaviour of these complexes. The significant structural alteration induced by substitution of thiophene for furan can be seen to account for the different redox behaviour of **3**. Hemico-ordination of thiophene sulphur in **3** could be considered to have thermodynamic and/or kinetic consequences in respect of redox reactivity. The potential five-co-ordination deriving from hemico-ordination of the pair of μ-thiophene donors would not constitute a favourable starting position for any mechanism involving co-ordination of dioxygen; normally accepted mechanisms[9] for Cu^I/O_2 autoxidation reactions involve a co-ordinatively unsaturated copper(I) site. To determine whether such an anticipated kinetic effect is the dominant factor determining the redox stability of **3**, electrochemical experiments were undertaken as described below.

Electrochemistry.—Because earlier[4] cyclic voltammetric studies of $[Cu_2L^1(MeCN)_2][ClO_4]_2$ **1** in dma or dmf had revealed irreversible behaviour, in this work we concentrated initially on the redox behaviour of the complexes in acetonitrile solution. The perchlorate complex $[Cu_2L^1(MeCN)_2][ClO_4]_2$ **1**, was used in preference to the BPh_4^- salt **1′** owing to the unsuitable nature of BPh_4^- for electrochemical studies.

At first, irreversible and poorly reproducible results were obtained in this solvent also until it was realised that solvent purity determined the quality of the voltammograms. The best results were obtained with freshly opened HPLC grade acetonitrile, handled under argon. Table 1 lists the electrochemical results obtained; in all three cases a pair of quasi-reversible waves was seen (Fig. 5) at positive potential (average value increasing in the order **2** < **1** < **3**). Although the oxidation wave of $[Cu_2L^4(NCMe)_2][ClO_4]_2$ was broad and tailed to less positive potential, a clearly resolved pair of waves was not seen. The significant observation, however, is that this wave was observed at *ca.* +1.0 V, *i.e.* a similarly positive

Table 1 Cyclic voltammetric data[a] in MeCN solution

Compound	$E^c(1)$	$E^a(1)$	$\Delta E(1)$	$E^c(2)$	$E^a(2)$	$\Delta E(2)$
1 $[Cu_2L^1(NCMe)_2][ClO_4]_2$[b]	596	720	124	993	1070	77
2 $[Cu_2L^2(NCMe)_2][ClO_4]_2$	479	603	124	908	1030	122
3 $[Cu_2L^3(NCMe)_2][ClO_4]_2$	821	961	140	1140	1250	110
4 $[Cu_2L^4(NCMe)_2][ClO_4]_2$[b]	966[c]	1060[c]	94			

[a] Potentials in mV *vs.* Ag–AgCl, scan rate 100 mV s^{-1}. Under these conditions, ferrocene showed a reversible wave at +401 mV *vs.* with a peak-to-peak separation of 59 mV. [b] This compound in addition showed an irreversible cathodic peak at *ca.* 300 mV. [c] One broad oxidation wave only.

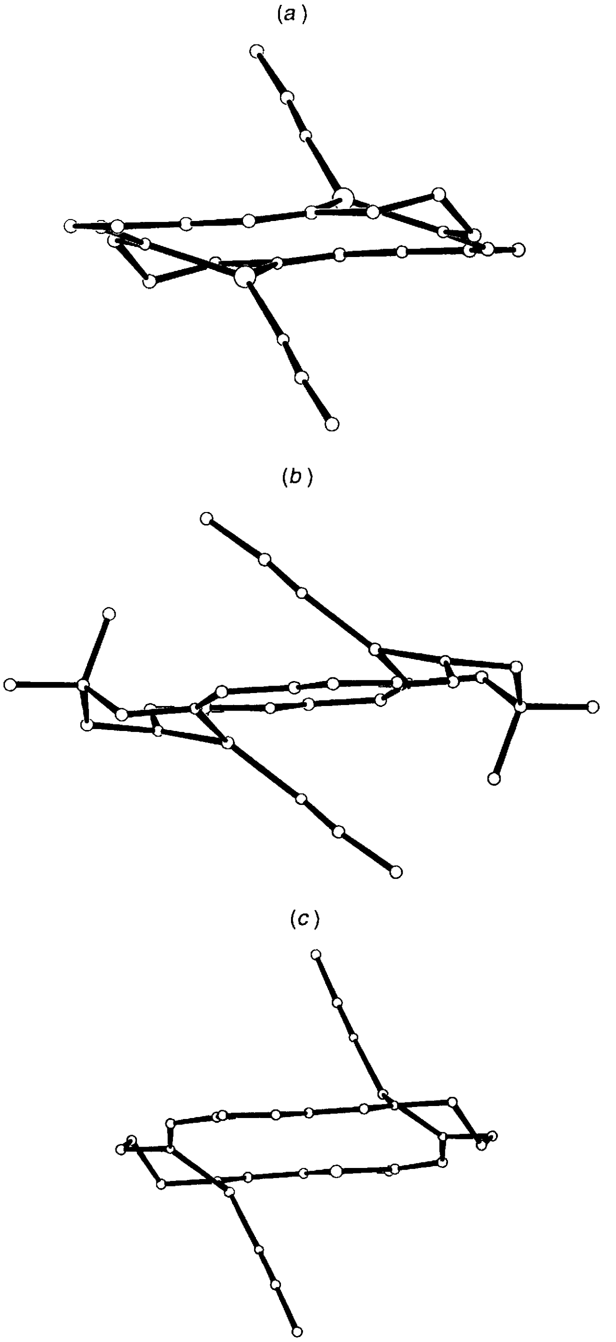

Fig. 4 The three cations projected onto the plane of the five-membered ring of the macrocycle

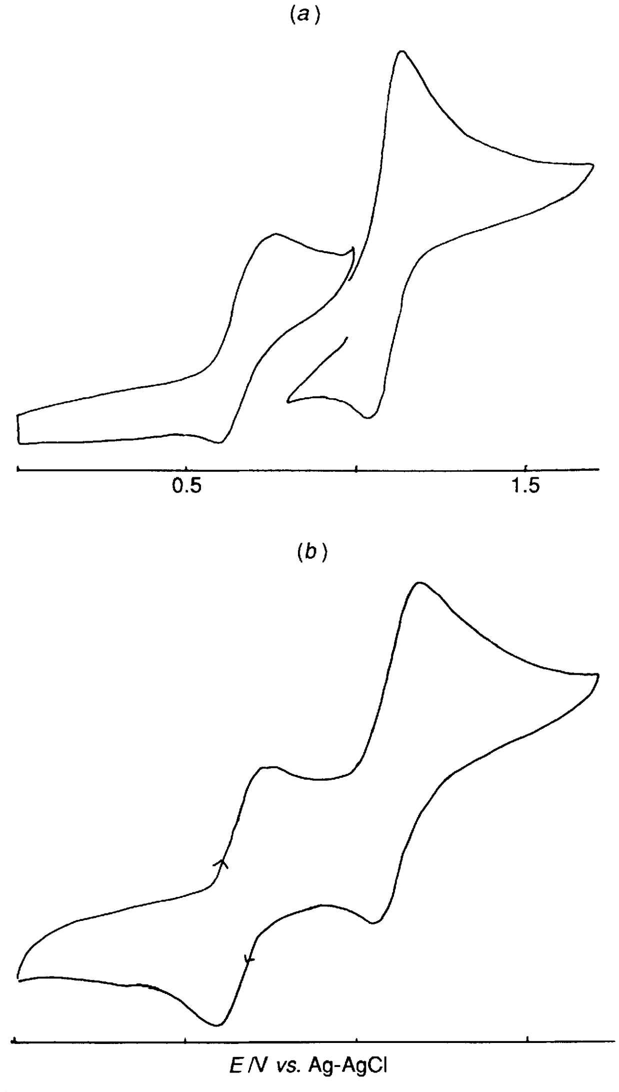

Fig. 5 Cyclic voltammograms of complex **2** in acetonitrile solutions (scan rate 100 mV s^{-1})

potential to the average of the pair of waves of **3**. As the Group 2 salts of these ligands were found to be electroinactive over the range studied, it seems a reasonable assumption to attribute the observed oxidation waves to metal-centred processes, very probably to sequential one-electron oxidations of the Cu^I_2 centres, as indicated in Scheme 1. The solubility of the complexes in acetonitrile (at $\leqslant 10^{-3}$ mol dm^{-3}) was too low for

$$Cu^I_2L \xrightarrow{-e} Cu^ICu^{II}L \xrightarrow{-e} Cu^{II}_2L$$

Scheme 1

meaningful coulometric measurements. However, as the relative intensity of the two waves seen for **1**–**3** was approximately equal, suggesting transfer of an equal number of electrons in each step, Scheme 1 is the most likely explanation of the redox behaviour in acetonitrile.

The first conclusion to be drawn from the data in Table 1 is

Table 2 Electrogeneration of mixed-valence species

Compound	Operating voltage[a]	No. electrons transferred	ESR parameters[b]	
			g	A_{iso}/G
1	650	0.94 ± 0.1	2.16	36
2	740	0.90 ± 0.1	2.16	35
3	850	1.17 ± 0.1	2.14	35

[a] In mV *vs.* SCE. [b] Assuming fourth line to be the centre of the irregular mixed-valence signal; G = 10^{-4} T.

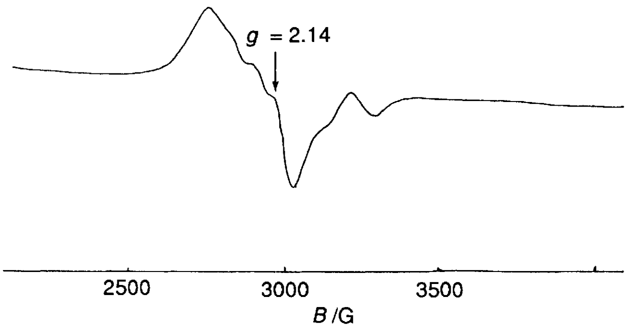

Fig. 6 The ESR spectrum of the electrogenerated mixed-valence form of complex **3** in dmf solution

that, in comparison with complexes **1** and **2**, **3** and **4** indeed have enhanced thermodynamic stability towards oxidation by O_2. Given the uncertainty about the nature and fate of the reduced O_2 species, comparison with standard redox potentials is of limited value. However, if the redox potential for O_2 under the conditions used for aerobic oxidation of **1** and **2** is not more positive than that of the $\frac{1}{2}O_2$–H_2O (aq) couple, it is likely that **3** and **4** have too high a first oxidation potential to be achievable by reduction of O_2. The second inference which can be made from the data for **1**–**3** is that the mixed-valence form is expected to have appreciable thermodynamic stability relative to the isovalent Cu^{II}_2 or Cu^{I}_2 state. Conproportionation constants of the order of 10^5–10^7 can be calculated from the relative $E_{\frac{1}{2}}$ values for electrochemical processes (1) and (2) (Table 1). Both of these conclusions are in agreement with chemical observation. It must be remembered, however, that the chemical observations relate to dma or dmf solutions, and that we have so far failed to generate any chemically oxidised mixed-valence or dicopper(II) form in acetonitrile solution. This may arise from kinetic factors deriving from blocking by MeCN solvate of the vacant co-ordination site needed for O_2 uptake.

We wished to compare the properties of the electrochemically generated mixed-valence forms of **1** and **2** with the chemically oxidised species already studied,[4] so preparative-scale electrochemistry was attempted. Unfortunately the solubility in acetonitrile was insufficient to permit successful electrogeneration experiments, so we were forced to use dmf for these experiments. Cyclic voltammetry of complex **1** in dmf had already shown[4] the oxidation wave to be irreversible; on the first scan a +590 mV anodic component [presumably the analogue of $E^a(1)$ in MeCN] has an associated cathodic wave, well separated at −145 mV, showing that some rapid change, possibly deco-ordination of MeCN solvate, follows upon oxidation. Coulometric measurements on *ca.* 10^3 mol dm^{-3} solutions of **1** indicate (Table 2) that the number of electrons transferred in the +590 mV oxidation step is approximately one; however attempts at exhaustive electrolyses designed to generate a pure mixed-valence species for *e.g.* UV or ESR spectroscopic examination reveal an *i vs. Q* plot which is non-linear over a 2-h period, flattening off after about 0.75 h. We believe that the electrogenerated species is not stable in dmf over the period of this experiment, and that some disproportionation process regenerating Cu^I accounts for the observation of electron counts greater than one in coulometric runs of more than 1 h duration. The ESR spectrum of the electrogenerated mixed-valence form of **1** supports this idea in that a g = 2.15 singlet suggestive of rapidly exchanging Cu^{II} is now quite dominant in the complex ESR pattern.[4] The spectra obtained by electrogeneration of the mixed-valence forms of **1** and **2** are similar (with the intensity change noted above) to those obtained by aerobic oxidation. The intensity of the spectrum reflects the extent of electrolysis, being around half that of a $Cu(ClO_4)_2·6H_2O$ standard for a half-electrolysed solution. (Solutions were of necessity only partially electrolysed.) The data are consistent with the formation of a one-electron paramagnet in the +590 mV oxidation process. Table 2 shows that a mixed-valence form of **3** could be obtained by electrochemical oxidation; its ESR spectrum (Fig. 6) was similar to those obtained for electrogenerated mixed-valence forms of **1** and **2**.

One striking and unforeseen difference between the electrogenerated and chemically generated mixed-valence forms was the absence from the electrogenerated form of the intense brown colour observed for the chemically generated form.

Argon-protected solutions containing the electrochemically oxidised form of complex **1** (present in about 1:1 ratio with unoxidised **1**) showed no development of the near-infrared absorption at *ca.* 850 nm and associated shoulder at *ca.* 480 nm until air was deliberately introduced, whereupon these bands started to grow in consequence of the interaction of O_2 with unoxidised **1**. A similar behaviour was observed with **2**, but, as expected, no brown colour or near-infrared absorption was observed on exposure of partly oxidised **3** to O_2.

Experiments with chemical oxidants did not result in development of the dark brown colour characteristic of aerobically oxidised complex **1**. Hydrogen peroxide and Br_2 generated the green dicopper(II) forms while the milder oxidant Ag^+ was slowly reduced to Ag(s) with concomitant development of an ESR signal similar to that of electrogenerated mixed-valence **1** but without appearance of the dark brown colour or absorption at 850 nm typical of aerobically oxidised $[Cu_2L^1]^{2+}$ in dmf.

The lack of an intervalence transfer band in the electronic spectrum of the electrogenerated mixed-valence species may mean that the latter lacks long-term stability or that a bridging oxo-donor is necessary for observation of this absorption. Certainly, other dicopper mixed-valence systems[10,11] for which intervalence transfer bands have been reported have had available an electron-transfer pathway *via* bridging oxygen. Under the conditions of the electrogeneration experiment (strict exclusion of water and O_2) there is unlikely to be any O-donor to provide such a pathway. The band at *ca.* 480 nm associated with the intervalence transfer absorption of aerobically oxidised complex **1** is reminiscent of $O_2^{2-} \longrightarrow Cu$ ligand to metal charge transfer.[12] Resonance-Raman experiments are planned[13] which may be able to confirm the presence of a μ-peroxo-dicopper species; in any case it seems clear that some co-ordinated μ-oxo-donor assists intervalence transfer between the copper ions in this case.

Experimental

Synthesis of Complexes.—Complexes **1′** and **2** were prepared as described earlier;[3] **3** was made either by transmetallation of $[CaL^3][ClO_4]_2$ or by direct condensation of 2,5-diformylthiophene and 1,3-diaminopropane analogously to the prepartion of $[Cu_2L^4(NCMe)_2][ClO_4]_2$ which follows.

$[CaL^3][ClO_4]_2$. 2,5-Diformylthiophene (0.5 g, 4.1 × 10^{-3} mol) and $Ca(ClO_4)_2·4H_2O$ (0.7 g, 2.3 × 10^{-3} mol) were dissolved in ethanol (15 cm^3) and heated to 40 °C. To this was added a solution of 1,3-diaminopropane (0.4 g, 5.4 × 10^{-3} mol) in ethanol (10 cm^3) and the resultant yellow solution stirred at room temperature for 1 h, during which time a white solid

Table 3 Crystal data and refinement details *

Compound	**1′**	**2**	**3**
Formula	$C_{70}H_{66}B_2Cu_2N_6O_2$	$C_{26}H_{34}Cl_2Cu_2N_6O_{10}$	$C_{22}H_{26}Cl_2Cu_2N_6O_8S_2$
M	1105.5	788.6	764.6
Crystal class	Monoclinic	Triclinic	Monoclinic
Space group	$P2_1/n$	$P\bar{1}$	$P2_1/c$
Absences	$h0l$: $h + l = 2n + 1$	—	$h0l$: $l = 2n + 1$
	$0k0$: $k = 2n + 1$	—	$0k0$: $k = 2n + 1$
a/Å	10.45(1)	7.447(8)	8.15(1)
b/Å	15.72(1)	12.094(9)	9.41(1)
c/Å	18.08(1)	10.731(9)	19.35(2)
α/°	(90)	118.6(1)	(90)
β/°	97.0(1)	78.8(1)	100.0(1)
γ/°	(90)	103.7(1)	(90)
Z	2	1	2
U/Å^3	2573	821	1462
F(000)	854	404	776
D_m/g cm^{-1}	—	1.69	—
D_c/g cm^{-1}	1.42	1.74	1.73
μ/cm^{-1}	15.85	26.49	31.02
Crystal size/mm	0.3 × 0.3 × 0.3	0.2 × 0.3 × 0.4	0.3 × 0.3 × 0.4
No. of data measured	3213	2768	2628
No. used in refinement	1122	1298	1071
Criterion for data inclusion	$[I > 2.5\sigma(I)]$	$[I > 3\sigma(I)]$	$[I > 2.5\sigma(I)]$
R	0.079	0.055	0.072
R′	0.084	0.061	0.077

* For all compounds: $\lambda = 0.7107$ Å; maximum $2\theta = 50°$

Table 4 Atomic coordinates (× 10^4) for complex **1′** with estimated standard deviations (e.s.d.s) in parentheses

Atom	*x*	*y*	*z*	Atom	*x*	*y*	*z*
Cu	5516(2)	4055(2)	5380(2)	C(24)	8784(17)	774(14)	4324(11)
N(1)	6804(17)	4831(10)	5117(8)	C(25)	8665(16)	47(13)	3918(12)
C(2)	7597(23)	5278(13)	5003(12)	C(26)	7650(23)	−41(13)	3375(12)
C(3)	8565(18)	5857(13)	4790(13)	C(31)	5265(17)	−378(12)	2197(11)
N(4)	4861(17)	2992(11)	4881(12)	C(32)	4223(19)	−905(15)	2171(10)
C(5)	4527(15)	2855(13)	4212(16)	C(33)	4233(21)	−1674(14)	1763(13)
C(6)	4509(16)	3447(14)	3636(15)	C(34)	5234(25)	−1909(14)	1386(13)
O(7)	4778(11)	4299(9)	3764(8)	C(35)	6240(22)	−1400(16)	1405(11)
C(8)	4713(16)	4681(19)	3112(15)	C(36)	6273(19)	−629(13)	1804(12)
C(9)	4939(17)	5601(19)	3065(17)	C(41)	5219(17)	1245(11)	2033(11)
N(10)	4895(20)	6124(14)	3600(11)	C(42)	6067(18)	1926(13)	1993(11)
C(11)	5175(25)	7025(18)	3416(15)	C(43)	5919(19)	2565(13)	1448(12)
C(12A)	4699(46)	7604(34)	3860(32)	C(44)	4876(26)	2550(13)	953(11)
C(12B)	5766(45)	7597(36)	3932(35)	C(45)	3955(20)	1893(15)	974(13)
C(13)	5220(29)	7748(13)	4582(17)	C(46)	4132(19)	1267(13)	1503(11)
C(14)	4268(19)	3332(14)	2895(14)	C(51)	4162(18)	588(12)	3165(11)
C(15)	4422(19)	4141(20)	2527(13)	C(52)	4293(15)	65(12)	3817(13)
B	5330(18)	531(14)	2662(11)	C(53)	3433(20)	78(12)	4304(12)
C(21)	6665(21)	568(13)	3231(9)	C(54)	2289(18)	565(16)	4204(15)
C(22)	6844(16)	1309(13)	3666(13)	C(55)	2173(17)	1094(14)	3586(15)
C(23)	7877(21)	1388(13)	4200(13)	C(56)	3045(18)	1067(12)	3086(12)

separated. Although satisfactory analyses were not obtained for this product, it could be used to prepare a pure sample of $[Cu_2L^3(NCMe)_2][ClO_4]_2$.

$[Cu_2L^3(NCMe)_2][ClO_4]_2$ **3**. The complex $[CaL^3][ClO_4]_2$ (0.2 g, 3.4×10^{-4} mol) was suspended in deoxygenated EtOH–MeCN (1:2) and the suspension heated to reflux. The salt $[Cu(MeCN)_4]ClO_4$ (0.2 g, 6.1×10^{-4} mol) was added and the yellow crystalline product isolated by frit filtration: yield 67%, Λ_m = 277 S cm^2 mol^{-1} (Found: C, 38.25; H, 4.30; N, 10.30. Calc.: C, 38.05; H, 4.20; N, 10.25%).

$[Cu_2L^4(NCMe)_2][ClO_4]_2$ **4**. 2,5-Diformylthiophene (1.0 g, 8.1×10^{-3} mol) and 2,2-dimethylpropane-1,3-diamine (0.8 g, 8.1×10^{-3} mol) were dissolved in deoxygenated ethanol (60 cm^3) at 60 °C. To this was added a solution of $[Cu(MeCN)_4]ClO_4$ (2.0 g, 6.1×10^{-3} mol) in hot, deoxygenated acetonitrile. The resultant orange solution was heated under argon for 15 min, during which time orange crystals of the product separated. These were isolated by frit filtration under Ar, washed with hot EtOH–MeCN (1:1, 5 cm^3) and dried with diethyl ether under Ar: yield 70%, Λ_m = 290 S cm^2 mol^{-1} (Found: C, 38.35; H, 4.25; N, 10.25. Calc.: C, 37.95; H, 4.40; N, 10.20%).

Crystallographic Measurements.—The complexes were recrystallised from MeCN. Crystal data are given in Table 3.

Intensity data were collected on a Stoe STAD12 diffractometer. Reflections were measured by ω scan with a scan speed of 0.0333° s^{-1}. Background counts at both ends of the scan were measured for 20 s. Absorption and extinction corrections were not applied. Densities were measured using the flotation method.

The positions of the metal atoms were determined from Patterson functions. Successive Fourier syntheses gave the

Table 5 Atomic coordinates ($\times 10^4$) for complex **2** with e.s.d.s in parentheses

Atom	*x*	*y*	*z*
Cu	6808(1)	−975(1)	−1068(1)
N(1)	6894(9)	251(9)	−1680(10)
C(2)	6887(10)	705(9)	2318(10)
C(3)	6583(17)	1296(17)	−3261(17)
N(4)	5651(9)	−2727(9)	−2335(9)
C(5)	4279(11)	−3222(12)	−3172(11)
C(6)	3102(10)	−2368(13)	−3098(12)
O(7)	3058(7)	−1181(8)	−1975(8)
C(8)	1886(9)	−649(10)	−2326(10)
C(9)	1527(8)	647(9)	−1357(12)
N(10)	1898(8)	1292(8)	−107(10)
C(11)	1317(11)	2587(10)	653(10)
C(12)	2746(11)	3660(10)	1324(11)
C(13)	3238(12)	3707(10)	2627(11)
C(14)	1938(11)	−2554(13)	−3936(12)
C(15)	1184(10)	−1473(11)	−3465(12)
C(16)	1946(15)	4889(13)	1840(15)
C(17)	4507(11)	3612(12)	272(14)
Cl	7566(3)	−2788(4)	3652(3)
O(19)	8093(16)	−3435(12)	4235(12)
O(20)	5784(11)	−2971(11)	3591(12)
O(21)	8613(17)	−3039(14)	2423(14)
O(22)	8160(31)	−1529(16)	4381(17)

Table 6 Atomic coordinates ($\times 10^4$) for complex **3** with e.s.d.s in parentheses

Atom	*x*	*y*	*z*
Cu	604(2)	534(2)	3897(1)
N(1)	969(14)	2425(16)	4148(6)
C(2)	1227(19)	3566(18)	4279(8)
C(3)	1669(23)	5037(18)	4451(11)
N(4)	2212(16)	−1019(13)	3827(8)
C(5)	3306(17)	−1606(15)	4265(8)
C(6)	3519(17)	−1398(16)	5004(8)
S(7)	2230(5)	−305(5)	5392(2)
C(8)	3337(18)	−618(17)	6199(8)
C(9)	2820(21)	−84(16)	6805(9)
N(10)	1289(15)	113(13)	6827(6)
C(11)	871(24)	799(16)	7458(8)
C(12)	−466(27)	1913(18)	7251(9)
C(13)	−2207(24)	1402(22)	6924(9)
C(14)	4718(17)	−1981(17)	5473(10)
C(15)	4684(16)	−1517(18)	6162(10)
Cl	3431(5)	−5801(5)	6445(2)
O(19)	4961(21)	−5300(19)	6360(12)
O(20)	3620(21)	−6515(18)	7068(8)
O(21)	2949(26)	−6736(20)	5919(8)
O(22)	2243(17)	−4728(17)	6424(8)

Table 7 Molecular dimensions (distances in Å, angles in °) in the metal co-ordination spheres, with e.s.d.s in parentheses

Complex	**1′**	**2**	**3**
Cu–N(1)	1.914(18)	1.872(13)	1.855(15)
Cu–N(4)	1.966(18)	1.978(8)	1.984(13)
Cu–N(10)*	1.966(21)	1.942(11)	1.991(11)
Cu • • • Cu*	3.395(4)	3.675(1)	4.654(3)
N(1)–Cu–N(4)	129.5(8)	115.2(4)	130.3(5)
N(1)–Cu–N(10)*	124.6(7)	140.1(3)	123.2(5)
N(4)–Cu–N(10)*	101.4(9)	101.4(4)	99.6(5)

* Atom in equivalent positions 1 − *x*, 1 − *y*, 1 − *z* for **1′**, 1 − *x*, −*y*, −*z* for **2** and −*x*, −*y*, 1 − *z* for **3** with respect to that at *x*, *y*, *z*.

Table 8 Macrocycle torsion angles (°) with e.s.d.s in parentheses

	1′ X = O	**2** X = O	**3** X = S
C(12A)*–C(13)*–N(4)–C(5)	173(3)	−137(1)	126(2)
C(12B)*–C(13)*–N(4)–C(5)	−134(3)		
C(13)*–N(4)–C(5)–C(6)	179(2)	−176(1)	180(1)
N(4)–C(5)–C(6)–X(7)	−6(3)	−17(2)	1(2)
C(5)–C(6)–X(7)–C(8)	178(2)	177(1)	−178(1)
C(6)–X(7)–C(8)–C(9)	179(2)	−179(1)	−175(1)
X(7)–C(8)–C(9)–N(10)	−17(3)	−13(1)	30(2)
C(8)–C(9)–N(10)–C(11)	179(3)	−178(1)	−174(2)
C(9)–N(10)–C(11)–C(12A)	157(3)	−127(1)	136(2)
C(9)–N(10)–C(11)–C(12B)	−148(3)		
N(10)–C(11)–C(12A)–C(13)	73(5)	−73(1)	68(2)
N(10)–C(11)–C(12B)–C(13)	−57(5)		
C(11)–C(12A)–C(13)–N(4)*	−64(6)	74(1)	−78(2)
C(11)–C(12B)–C(13)–N(4)*	62(5)		

* Atom in equivalent position given in Table 7.

Table 9 Least-squares planes for atoms N(4)–N(10) inclusive. Equations are in the form $AX + BY + CZ = D$, where X, Y and Z are the cartesian co-ordinates.

	1′	**2**	**3**
A	0.99	0.71	0.42
B	−0.11	0.28	0.89
C	−0.12	−0.64	−0.16
D	3.39	−0.33	−1.35
Distances (Å) from planes (e.s.d. *ca.* 0.01 Å)			
Cu	0.49	0.90	0.79
N(4)	0.10	0.16	0.09
C(5)	−0.08	−0.12	−0.14
C(6)	−0.08	−0.06	−0.13
O(7)	0.03	−0.06	0.20
C(8)	0.04	0.09	0.08
C(9)	0.12	0.14	0.15
N(10)	−0.12	−0.14	−0.25
C(14)	−0.15	−0.05	−0.33
C(15)	−0.05	0.05	−0.17

position of the remaining atoms. Two possible positions were located for C(12) in complex **1′**; these were both given a fixed occupancy of 0.5 and denoted by C(12A) and C(12B). Hydrogen atoms were fixed in trigonal or tetrahedral positions. Those in **1′** were given a fixed thermal parameter of 0.07 Å^2 which was not refined, and no attempt was made to include hydrogens on the disordered atoms. In **2** and **3**, hydrogens bonded to the same atom were given a common thermal parameter which was refined. In **2** this was set equal for the hydrogens bonded to C(14) and C(15). Structure **1′** was refined using block-matrix least squares, the cation and anion being refined in alternate cycles. Full-matrix least squares was used for the other two structures. All non-hydrogen atoms were refined anisotropically and all hydrogen atoms isotropically, except for the disordered atoms in **1′** which remained isotropic. The weighting scheme was chosen to give similar values of $w\Delta^2$ over ranges of $\sin\theta/\lambda$ and F_o, $w = 1/[\sigma^2(F) + 0.003F^2]$. The final Fourier difference maps showed no significant peaks. In all structures the final shift/error ratio in the refinement was less than 0.1:1.

Calculations were performed on the University of Reading Amdahl V7 computer using SHELX 76.[14] Atomic scattering factors were taken from ref. 15 together with corrections for anomalous dispersion. Final positional parameters for complexes 1, 2 and 3 are given in Tables 4, 5, and 6 respectively. Dimensions in the metal co-ordination spheres are listed in Table 7, Table 8 gives the macrocycle torsion angles and Table 9 lists the least-squares planes for each structure.

Additional material available from the Cambridge Crystallographic Data Centre comprises H-atom coordinates, thermal parameters and remaining bond lengths and angles.

Cyclic Voltammetry.—Cyclic voltammetry measurements were carried out using an EG and G PAR model 362 potentiostat, in conjunction with a three-electrode cell fitted with a purge-gas inlet and outlet and consisting of a platinum-wire working electrode, a Ag–AgCl reference electrode and a platinum auxiliary electrode. The voltammograms were recorded from *ca.* 10^{-3} mol dm^{-3} solutions of the copper complex in MeCN (HPLC grade) containing about 0.2 mol dm^{-3} NBu_4ClO_4. These voltammograms were recorded in a Linseis LY 1800 X-Y recorder. The data (E_p^a, E_p^c; iR_n compensation) were processed using the convolution transform technique.

Controlled-potential Electrolysis.—The following solvents were used for coulometric and electrogeneration studies: acetonitrile HPLC grade was dried with molecular sieves (evacuated at 400 °C before use); dmf and dma were dried with anhydrous $CuSO_4$ and distilled under reduced pressure over N_2 and dried with molecular sieves. Tetraethylammonium perchlorate as an electrolyte was used as supplied by Fluka without further purification.

All electrochemical studies were performed with a three-electrode potentiostatic system. The working electrode was a platinum plate (10 × 5 mm), platinum wire formed the counter electrode and the reference electrode was a silver wire which showed a potential of 0.46 V *vs.* the saturated calomel electrode (SCE). Oxidations were performed by stepping up the anode potential to 1.1 ↔ 1.3 V *vs* silver wire and collecting the current transient over 10 s. The potentiostat was a PAR 176 model with 274 digital interface and controlled through an Apple IIe computer. The solutions were *ca.* 5×10^{-3} mol dm^{-3} in dmf or dma with 0.1 mol dm^{-3} tetraethylammonium perchlorate as an electrolyte. They were degassed with argon and oxidation was carried out at 15 °C under an atmosphere of argon for periods of 30 min–2 h. The UV spectrum was run on an electrolysed solution transferred using a cannula under argon, to a 5 mm cell, degassed with argon. The ESR spectra were run in a 1 mm capillary cell on solutions transferred in the same way.

Spectral Measurements.—Electronic spectra were recorded using a PEDλ 9 IR–UV–visible spectrometer, ESR spectra with a Varian E109 spectrometer. Proton NMR were run at 250 MHz using a Bruker WM 250 instrument. Complexes **3** and **4** in CD_3CN both exhibited singlets at δ 7.51 corresponding to the thiophene proton, and at 8.43 and 8.36 to the imino-proton (in **3** and **4**, respectively). The methylene protons α to the imino N occurred in **3** as a triplet at δ 4.03 and in **4** as a singlet at δ 3.81. The β-methylene signal of **3** was obscured by solvent peaks but the methyl signal of **4** could be seen as a singlet at δ 0.90.

Acknowledgements

We thank the SERC and Department of Education, Northern Ireland for studentships (to P. C. Y. and K. P. Mc.K.) and a fellowship (to J. T.-G.), A. W. Johans for his assistance with the crystallographic investigations and the SERC for part-funding the ESR spectrometer and the PEλ 9 UV spectrophotometer.

References

1 S. M. Nelson, J. T.-Grimshaw, A. Lavery, K. P. McKillop and M. G. B. Drew, in *Biological and Inorganic Copper Chemistry*, eds. K. D. Karlin and J. Zubieta, Adenine Press, New York, 1985.
2 M. G. B. Drew, A. Lavery, F. S. Esho and S. M. Nelson, *J. Am. Chem. Soc.*, 1983, **105**, 5693.
3 M. G. B. Drew, P. C. Yates, J. T.-Grimshaw, A. Lavery, K. P. McKillop, S. M. Nelson and J. Nelson, *J. Chem. Soc., Dalton Trans.*, 1988, 347.
4 M. F. Cabral, J. Cabral, J. T.-Grimshaw, K. P. McKillop, S. M. Nelson and J. Nelson, *J. Chem. Soc., Dalton Trans.*, 1989, 1351.
5 K. P. McKillop, Ph.D. Thesis, Queens University of Belfast, 1988.
6 P. C. Yates, Ph.D. Thesis, University of Reading, 1986.
7 C. R. Lucas, S. Liu, M. J. Newlands, J. P. Charland and E. J. Gabe, *Can. J. Chem.*, 1989, **67**, 639.
8 G. C. van Stein, G. van Koten, K. Vrieze, A. L. Spek, E. A. Klop and C. Brevard, *Inorg. Chem.*, 1985, **24**, 1367.
9 K. D. Karlin, R. W. Cruse, Y. Gultneh, J. C. Hayes, J. W. McKown and J. Zubieta, in *Biological and Inorganic Copper Chemistry*, eds. K. D. Karlin and J. Zubieta, Adenine Press, New York, 1985.
10 R. C. Long and D. N. Hendrickson, *J. Am. Chem. Soc.*, 1983, **105**, 1513.
11 R. R. Gagné, L. M. Henling and T. J. Kistenmacher, *Inorg. Chem.*, 1980, **19**, 1226; R. R. Gagné, C. A. Koval, T. J. Smith and M. C. Cimolino, *J. Am. Chem. Soc.*, 1979, **101**, 4571.
12 E. Asato, S. Hashimoto, N. Matsumoto and S. Kida, *J. Chem. Soc., Dalton Trans.*, 1990, 1741.
13 J. J. McGarvey and J. Nelson, unpublished work.
14 G. M. Sheldrick, SHELX 76, Program for Crystal Structure Determination, University of Cambridge, 1976.
15 *International Tables for X-Ray Crystallography*, Kynoch Press, Birmingham, 1974, vol. 4.

Received 8*th January* 1991; *Paper* 1/00091H